



Islamic Azad University  
Mashhad Branch

# **Geochemical evolution and petrogenesis of the Eocene Kashmar granitoid rocks, NE Iran: implications for fractional crystallization and crustal contamination processes**

**Rahim Dabiri<sup>\*1</sup>, Mohsen Akbari-Mogaddam<sup>2</sup>, Mitra Ghaffari<sup>3</sup>**

*1. Department of Geology, Mashhad Branch, Islamic Azad University, Mashhad, Iran*

*2. Geological Survey of Iran, North- East Territory, Mashhad, Iran*

*3. Department of Geology, Tarbiat Modares University, Tehran, 14115-175, Iran*

Received 10 April 2016; accepted 17 October 2017

## **Abstract**

Kashmar granitoids of Taknar zone, in north part of Lut block, intruded into volcanic rocks and consist of granites, granodiorites, monzodiorite and gabbrodiorites. They are composed of mainly plagioclase, alkali-feldspar, quartz, amphibole, biotite and pyroxene minerals. Harker diagram variation, including negative correlations CaO, MgO, FeO, TiO<sub>2</sub> and V and positive correlations K<sub>2</sub>O, Rb, Ba, and Th, with increasing SiO<sub>2</sub> and chondrite-normalized REE patterns, suggest that fractional crystallization of gabbrodioritic rocks could have played a significant role in the formation of granites. Their chondrite-normalized REE patterns are characterized by LREE enrichment and show slight negative Eu anomalies. Chondrite-normalized REE modelling indicates that the magma of Kashmar gabbrodiorites were generated with 3–5% of partial melting of a spinel-lherzolite source. Melting of parental magma located at ~53 km.

**Keywords:** *Petrogenesis, Geochemical Modeling, Contamination, Granitoids, Taknar Zone*

## **1. Introduction**

The geology of Central and Eastern Iranian terrains is immensely complicated because of the collision between the micro-continents and overprinting of many metamorphic and tectonic events (Stöcklin and Nabavi 1972) as a result of continuous continental deformation in response to the ongoing convergence between the Arabian (Gondwana) and Turan (Eurasian) plates (Monazzami Bagherzadeh et al. 2015). Taknar zone is an exotic block that formed north part of Lut block (NE Iran) and surrounded by Daruneh and Taknar faults. It is located to the north of the Kashmar- Kerman volcano-plutonic arc (Fig 1). It is narrow upcoming rocks consist of metamorphic and sedimentary unites with Precambrian and Paleozoic age and overlaying Mesozoic and Cenozoic rocks. The Taknar zone granitoids are composed of two major plutons including Bornavard and Kashmar granitoids. Kashmar and Bornavard granitoids surrounded by taknar formation and volcanic and pyroclastic rocks respectively. North Kashmar granitoids with respect to characteristics of Alborz and Sabzevar magmatism suggested as Neothetys back- arc basin (Asiabanha and Foden 2012; Alaminia et al. 2013). Rb-Sr geochronological study on Kashmar granitoids showed that they have formed in

Middle Eocene time (Soltani 2000; Shafaii Moghadam et al. 2015). The aim of this paper is to demonstrate the source and petrogenesis of Kashmar granitoid rocks using geochemical modeling.

## **2. Geological setting**

Kashmar region granitoids outcrop for ~100 km and occupy the eastern part of Taknar zone. They are younger in age than some Bornavard (Precambrian) granitoids and have Eocene age (Soltani 2000; Shafaii Moghadam et al. 2015) (Fig 2). The contact of the granitoids with the surrounding rocks is either faulted or narrow hornblende-hornfelsic rims which have developed in the Eocene volcanic rocks. Granitoid rocks of Kashmar include granites, granodiorites, monzodiorite and gabbrodiorites. Granites intruded into inner parts of this pluton and are relatively younger than granodiorites and monzodiorite. Granites are most frequent granitoid rock in Kashmar area. Field observations show that granites are medium grain, equigranular and light grey. These rocks have hypidiomorphic granular and in marginal portions glomeroporphyry textures. Mafic microgranular enclaves (MMEs) with igneous textures are present in granodiorites and monzodiorite.

\*Corresponding author.

E-mail address (es): [r.dabiri@mshdiau.ac.ir](mailto:r.dabiri@mshdiau.ac.ir)

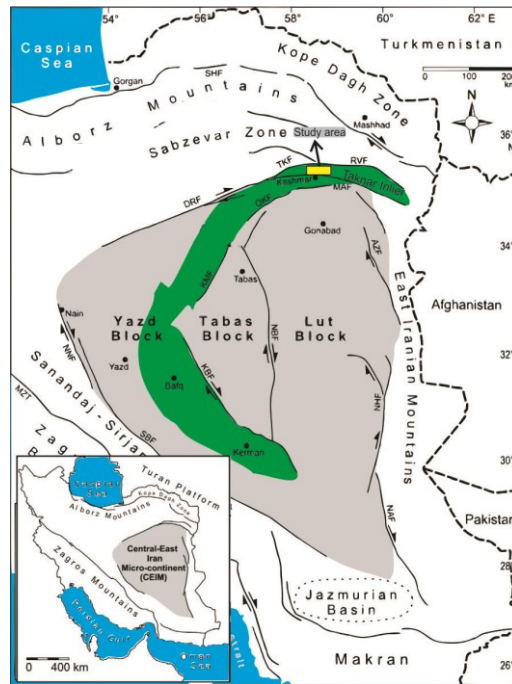


Fig 1. Simplified tectonic map of Central-East Iran and its constituent crustal blocks containing important faults, as well as the location of the study area, i. e., the Kashmar-Kerman volcano-plutonic arc shown in green color (compiled from Alavi (1991); Ramezani and Tucker (2003).

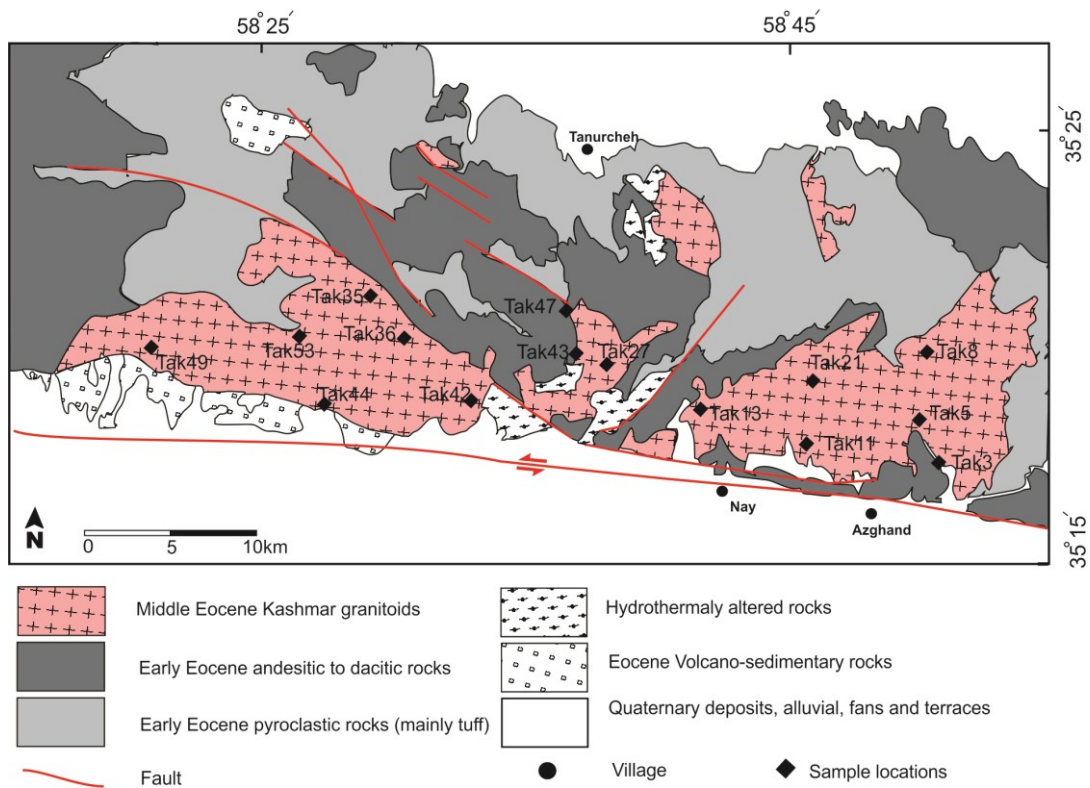


Fig 2. Simplified geological map of the Kashmar granitoids showing sample localities (modified after Kashmar and Feyzabad 1/100000 maps).

Most MMEs have circular shapes and are 3 to 4 cm in dimensions. They have also sharp boundary with granodiorites and monzodiorite. To the east of Taknar zone gabbrodiorites in small volumes are present.

### 3. Field observations and Petrography

Granites of Kashmar area are most widespread rock-type the district. Sometimes these rocks have been cut by granodioritic dikes (Fig 3a). It is light gray in color, medium-grained (3-5mm) and equigranular to porphyritic in texture. It consists essentially of plagioclase, alkali-feldspar, quartz, amphibole and biotite crystals. The accessory minerals include titanite, zircon and apatite. The plagioclase is fine to medium grained and subhedral to euhedral. It is zoned and altered into sericite. The alkali-feldspar is medium to coarse grained and shows perthitic and graphic textures (Fig 3a). Quartz occurs as filling within the interstitial spaces of the minerals. Amphibole grains occur either as prismatic crystals. They have been variably converted to biotite. Biotite is fine to medium grained and occurs as prismatic crystals that show pale green to brown pleochroism. The accessory minerals like titanite, zircon and apatite are fine grained and also occur as inclusions within the essential minerals.

The granodiorites are fine to medium grained, and composed mainly of plagioclase, quartz, amphibole, biotite and alkali-feldspar (Fig 3c). Plagioclase constitutes an average of 40% by volume of the rock, ranging from 35% to 65%. Quartz and alkali-feldspar are interstitial, or occur as interlocking anhedral grains. They usually have hypidiomorphic granular texture, but

some samples indicate alotriomorphic granular texture. Microgranular enclaves are common in granodiorites. Most of them are spherical in shape and 4-5 cm in size. Enclaves are rich plagioclase, amphibole, apatite and zircon and seem to be mineralogically related to the host rocks.

The Kashmar monzodiorite is composed essentially of sodic plagioclase, quartz, alkali feldspar and mafic minerals (hornblende and biotite). These rocks have a holocrystalline granular texture (Fig 3d). Plagioclase varies from 45 to 55% of the rocks and forms subhedral to euhedral crystals; it is generally zoned and exhibits variable degrees of alteration. The alkali feldspar occurs in perthitic form as Carlsbad twins. Usually it is a pure orthoclase but it may be intermediate and rarely kaolinitized. The gabbrodiorites are fine to medium grained, and composed mainly of clinopyroxene (15–20%), plagioclase (65–70%) and biotite (5%). In most cases, pyroxenes and plagioclases are similarly euhedral to subhedral, suggesting coprecipitation of the two phases. Pyroxenes usually have reaction rims of biotite and hornblende. Accessory minerals include magnetite, ilmenite and stubby apatite. Clinopyroxene grains from the gabbrodiorites show complicated compositional zoning.

### 4. Analytical techniques

A total of about 40 samples from the Taknar zone granitoids were collected. Sixteen representative samples were then selected for whole rock chemical analysis (Table 1).

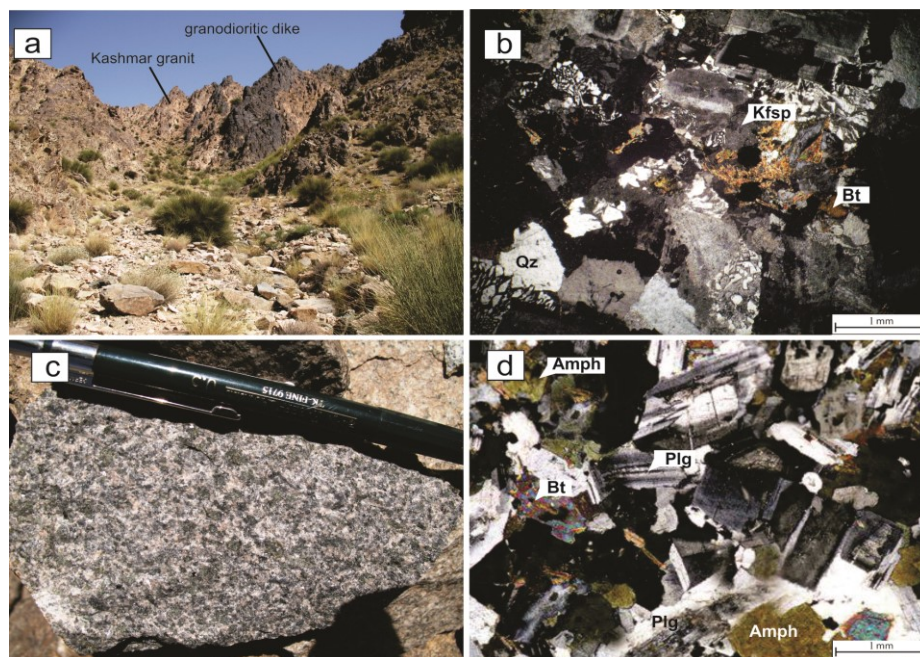


Fig 3. (a) granodioritic dike intruding Kashmar granitoids (b) Crossed polar photomicrograph of Kashmar granites with granophyric intergrowths of alkali-feldspar (Kfsp) and quartz (Qz), (c) Field photograph of the granodioritic rocks, (d) Plagioclase (Plg), Amphibole (Amph) and biotite (Bt) assemblages in monzodiorites.

Table 1. Whole rock geochemical data from the North Kashmar intrusions (Oxides, wt% and traces, ppm)

Sample	Tak 3	Tak 5	Tak 8	Tak 11	Tak 13	Tak 21	Tak 27	Tak 35	Tak 36	Tak 42	Tak 43	Tak 44	Tak 47	Tak 49	Tak 53	Tak 62
SiO <sub>2</sub>	60.09	67.22	68.28	59.31	65.03	58.47	67.61	65.61	66.56	63.43	54.48	64.41	54.65	69.53	70.33	58.21
Al <sub>2</sub> O <sub>3</sub>	17.2	16.5	15.91	16.74	16.42	16.18	16.05	16.65	16.45	17.22	17.5	16.68	17.74	15.71	15.5	16.13
Feo	6.81	4.03	3.92	7.68	4.76	8.04	4.29	4.68	4.48	5.03	9.55	4.97	7.74	3.25	3.17	7.15
MgO	2.15	1.32	1.26	2.8	1.64	3.67	1.38	1.78	1.63	1.99	4.31	1.79	3.01	1.05	1.03	2.92
CaO	5.17	3.41	3.09	4.3	3.45	5.33	3.1	2.95	3.81	3.87	4.22	3.31	7.62	2.67	2.72	5.5
Na <sub>2</sub> O	4.35	3.72	3.74	4.17	3.81	3.31	3.81	3.81	3.75	3.78	3.83	3.79	3.5	3.77	3.8	3.23
K <sub>2</sub> O	2.28	3.58	3.71	2.89	3.64	2.94	3.34	3.54	2.83	3.43	1.67	3.46	1.38	3.72	3.54	3.04
TiO <sub>2</sub>	1.01	0.55	0.55	0.91	0.61	0.89	0.56	0.6	0.6	0.63	0.9	0.63	0.83	0.51	0.49	0.85
P <sub>2</sub> O <sub>5</sub>	0.36	0.15	0.15	0.24	0.17	0.24	0.16	0.19	0.16	0.18	0.23	0.18	0.21	0.15	0.14	0.24
MnO	0.17	0.09	0.09	0.13	0.13	0.12	0.13	0.12	0.11	0.14	0.13	0.14	0.14	0.08	0.07	0.16
LOI	0.07	0.04	0.07	0.76	0.84	0.01	0.09	0.61	0.06	0.99	1.74	1.08	2.6	0.01	0.06	0.12
Rb	52	92.2	96	62	98	81	87	93.2	66	85	79	96.2	66	93	84	58
Ba	468	590	558	518	545	343	550	545	653	600	308	574	223	634	624	405
Sr	384	307	302	380	367	321	333	358	332	378	332	367	383	322	285	335
Pb	6	11	9	10	15	10	9	12	8	18	6	17	8	8	7	8
Th	5.65	12.98	9.97	11.72	9.44	7.65	9.97	10.15	9.98	9.13	3.32	9.32	4.33	10.68	11.58	4.13
Zr	167	211	222	155	186	154	222	210	190	180	95	186	109	231	232	158
Hf	5.3	6.1	5.44	5.6	5.5	7.1	5.45	5.7	5.1	5.3	5.5	5.1	5.1	5.7	5.2	6.6
Ta	1	1	0.27	0.9	0.27	0.7	0.9	0.9	0.9	0.28	0.9	0.9	0.7	0.28	0.27	0.4
Y	33	26	26	35	24	19	24	24	25	23	22	23	24	27	27	9
Nb	10.1	9.8	9.4	8.8	9.5	3.1	9.4	9.4	9.2	9.1	4.9	9.3	6.6	9.2	9.6	2.3
Cr	8	14	22	6	29	13	24	24	24	24	22	24	12	19	24	9
Ni	5	7	7	6	10	7	8	9	8	10	7	9	3	5	6	5
Co	7.6	6.6	7.1	9.7	8.6	9.3	7.7	6.6	8.6	9.3	8.4	9	8.5	7.4	5.3	8.1
V	155	82	80	201	106	205	92	104	104	109	231	109	199	73	16	176
Ga	18.22	16.42	18.12	18.92	16.42	20.32	17.22	18.42	16.32	16.32	19.22	17.22	18.52	16.32	17.22	17.82
La	28	30	29	30	33	25	29	32	30	28	10	28	13	28	29	21
Ce	63	60	59	68	63	56	58	64	60	65	21	55	25	58	59	41
Pr	6.89	6.36	5.61	6.74	6.82	6.3	6.07	6.75	6.36	6.84	3.21	5.84	3.71	5.47	5.04	7.35
Nd	20.7	22.6	22	23.1	24	23.3	22	23.7	23	24.6	15.4	21.3	16.8	21.4	20.61	21.6
Sm	4.52	4.67	4.69	4.79	4.45	4.28	4.23	4.55	4.62	4.29	2.5	4.31	2.7	4.76	4.66	4.7
Eu	1.04	0.96	1.03	1.02	1.06	1.08	1.01	1.06	1.08	1.05	0.41	1.05	0.52	1.03	1.05	1.06
Gd	4.77	5.3	5.13	4.95	5.28	5.5	5.12	5.29	5.29	5.1	3.4	4.93	3.5	5.14	5.13	5.1
Tb	0.7	0.7	0.67	0.68	0.69	0.65	0.66	0.66	0.72	0.67	0.52	0.65	0.44	0.7	0.67	0.67
Dy	5.32	4.24	4.27	4.52	4.05	4.21	4.02	4.08	4.24	3.99	2.77	4.01	3.01	4.25	4.28	4.28
Ho	0.83	0.83	0.85	0.81	0.81	0.83	0.82	0.82	0.86	0.79	0.64	0.79	0.69	0.83	0.83	0.78
Er	3.11	2.57	2.46	3.07	2.32	2.91	2.36	2.41	2.51	2.29	2.9	2.29	3.1	2.36	2.59	2.78
Tm	0.35	0.42	0.38	0.37	0.4	0.39	0.38	0.38	0.4	0.39	0.25	0.38	0.22	0.47	0.39	0.4
Yb	2.91	3.02	2.65	3.08	2.03	2.74	2.37	2.44	2.84	3.42	2.82	2.28	2.91	2.43	2.25	2.42

Samples weighed between 1–1.5 kg before crushing and powdering. Whole-rock major elements were determined by X-ray fluorescence spectrometer (XRF) and trace and rare earth elements (REE) were determined by Lithium metaborate fusion ICP-MS at the SGS laboratory in Toronto, Canada.

## 5. Geochemistry

The whole-rock major, trace and rare earth element composition of the Kashmar granitoids is given in Table 1. Kashmar Granitoids ranges in composition from gabbrodiorite to granite in TAS diagram (Cox et al. 1979), in which they have a subalkaline affinity (Fig 6). The Harker diagrams show a negative correlation of SiO<sub>2</sub> with CaO, MgO, FeO, TiO<sub>2</sub>, and V, and a positive correlation with K<sub>2</sub>O, Ba, Rb and Th (Fig 5). Such compositional variations of the rocks on Harker diagrams shows that the chemical compositions are constrained by crystal fractionation dominated by ferromagnesian phase(s) (pyroxene, amphibole) and plagioclase. In the primitive mantle-normalized (Sun and McDonough 1989) trace element patterns (Fig 6), all of the Kashmar granitoids show enrichment in large-ion lithophile elements (LILEs such as Rb, Sr, and K) relative to high-field strength elements (HFSEs) (i.e. Nb, Ta, P, Ti) and heavy rare earth elements (HREEs). Chondrite-normalized rare earth element (REE) patterns for the Kashmar granitoids are all LREE-enriched relative to heavy rare earth elements (HREEs) with (La/Yb)<sub>n</sub>=2.4-10.9 (Fig 6b). They have a negative Eu anomaly and relatively flat HREE pattern. The moderately HREE depletion may indicate the presence of garnet in the melt residue. Gabbrodiorites have low total REE contents relative to other samples and show a stronger negative Eu anomaly.

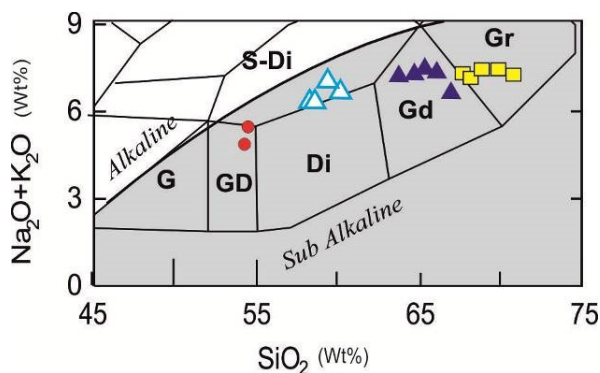


Fig 4. Total alkalis versus silica (TAS) discrimination diagram after Cox et al. (1979) for the classification of the Kashmar granitoids.

## 6. Discussion

### 6.1. Magma generation and geochemical modeling

The composition of the parental magma for the Kashmar granitoid rocks were estimated from the composition of most primitive gabbrodioritic sample (Tak43). This sample which has high FeO, MgO, Co

and Ni contents (9.55 wt%, 4.31 wt%, 8.40 and 7.0 ppm, respectively), can be candidate as parental magma for the evolved rocks (Wilson 1989a). The derivation of granites by fractional crystallization from the more basic magma (Tak43) was modeled geochemically. Numerical calculations for fractional crystallization of plagioclase, K-feldspar, quartz, biotite and amphibole (Pl/Kf/Q/Bi/Amp= 45:20:20:10:5) from the gabbrodioritic initial magma using rare earth elements was also carried out. The results obtained from 20% to 90 % degree of fractional crystallization modeling of Tak43 sample were compared to the granitic samples on the chondrite normalized spidergram (Fig 7). It is clear in Figure 7 that the rare earth element pattern obtained from the 40 % fractional crystallization of the Tak43 sample has the highest similarity to the granitic samples. The Rayleigh fractionation law (Hanson 1978; Hanson 1980) and partition coefficients after Rollinson (1993) were used in these calculations.

### 6.2. Role of crustal contamination

In order to constrain the role of crustal contamination, we have utilized some diagrams using major, trace and rare earth elements. On the Nb/Th vs. Nb/La diagram, all samples have a positive correlation of Nb/La and Nb/Th, and are consistent with crustal assimilation (Fig 8). On the other hand, the granitoids in the Kashmar area have restricted Nb/Th against highly variable Nb/La, indicating insignificant crustal contamination (Fig 8a). LILE such as Pb is commonly enriched in magmas that have undergone crustal assimilation (Fig. 8b). Measured ratios of Ce/Pb for primary mantle derived liquids are  $25 \pm 5$  (Hofmann et al. 1978; Sun and McDonough 1989). The least mobile high field strength element (HFSE) is positively correlated to Pb and Ce, suggesting that these elements have not been mobilized by others processes such as weathering. Ce/Pb ratios for most of the Kashmar granitoids (Fig 8b) are  $< 25 \pm 5$ , suggesting that magmas of Kashmar granitoids underwent copious crustal contamination. We have also prepared Th/Yb versus Nb/Yb diagram to determine the crustal contamination of Kashmar granitoids (Fig 8c). Th is more affected than Ta and Yb during crustal contamination processes. So, the rocks which affected by crustal contamination show high Th/Yb values (Wilson 1989b). The composition of the upper crust has also been plotted on the diagram.

### 6.3. Determination of source characteristics

The behavior of trace and rare earth elements during melting of mantle peridotite is affected by their partitioning coefficient in which they are moderately incompatible (Katz et al. 2003; Sobolev et al. 2007). So their concentrations and ratios are not greatly affected by mantle depletion and fluid influx (Pearce and Peate 1995; Munker 2000; Schmädicke et al. 2015).

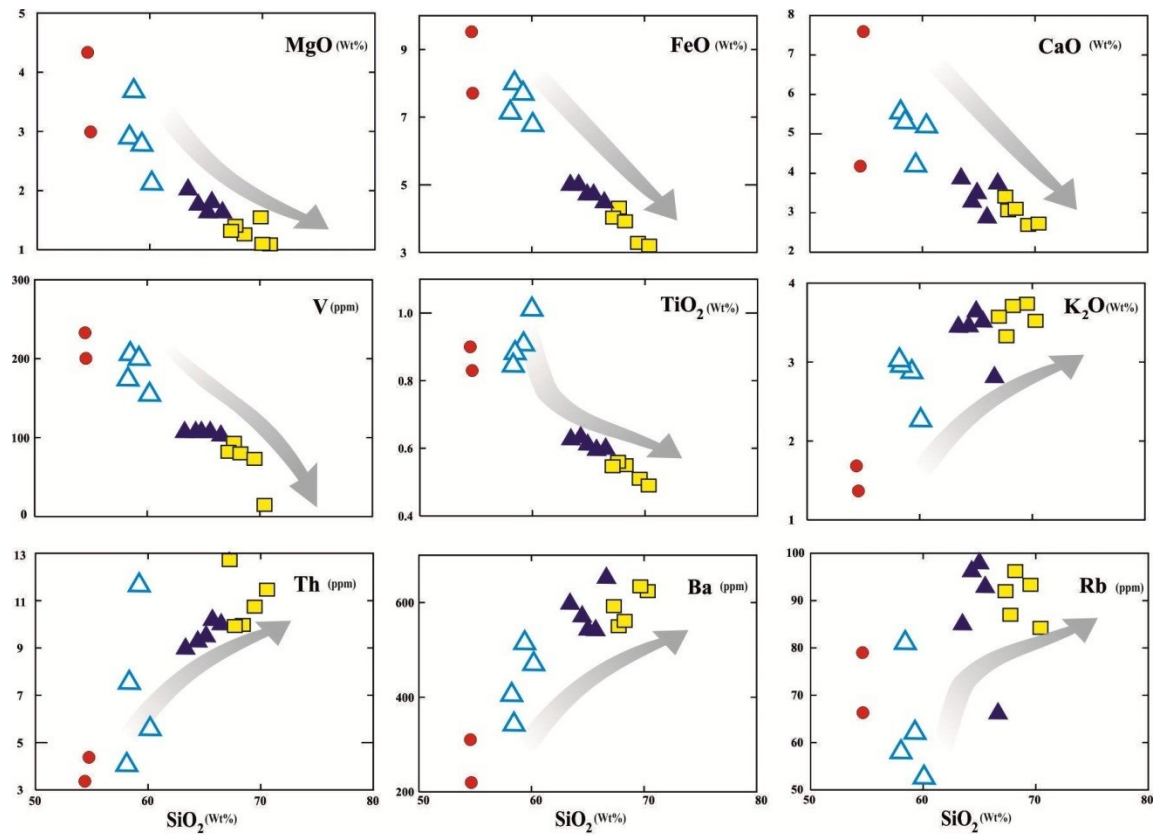


Fig 5. Harker variation diagram of some major oxide and trace element contents for the Kashmar granitoids, (symbols as for Figure 4).

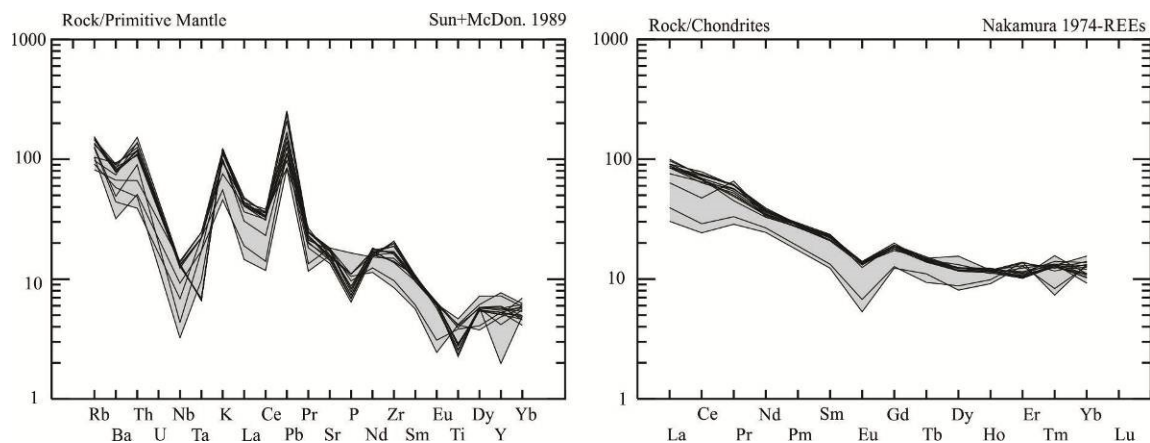


Fig 6. Normalized multi-element plots ('spider diagrams') and REE plots. (a) Primordial mantle normalized spider diagrams for representative Kashmar granitoids. Normalizing values are from Sun and McDonough (1989). (b) REE-chondrite normalized diagrams for the Kashmar granitoids. Normalizing values are from Nakamura (1974).

These elements are mainly controlled by mantle compositions and degrees of partial melting and are useful to determine the degrees, variations of mantle melting and origin of the magmas (Gurenko and Chaussidon 1995; Johnson 1998; Munker 2000; Green

2006; Zhao and Zhou 2007). So we can utilize them in evaluating residual mineralogies and degrees of partial melting. Subsequently, we have carried out REE modeling of the Kashmar granitoid rocks using the partial melting equations of (Shaw 1970) and the REE

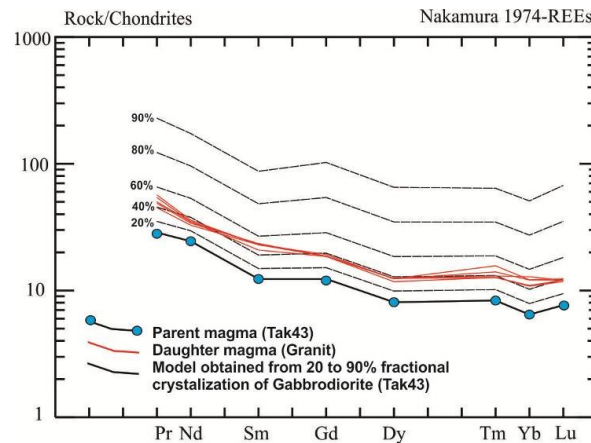


Fig 7. Fractional crystallization modelling of the rare earth elements (REEs) of the Kashmar granitoids. Chondrite-normalized REE diagrams (Nakamura 1974) calculated from the parental gabbrodiorite magma (Tak43) at 20–90% fractional crystallization, compared with the daughter magma (Granit samples). The mineral composition of parent magma consists of 45% plagioclase, 20% K-felspar, 20% quartz, 10% biotite and 5% amphibole. The models assume fractional crystallization (FC) and use partitioning coefficients from McKenzie and O'Nions (1991) for Plg and Amph, and Fujimaki et al. (1984) for Bio.

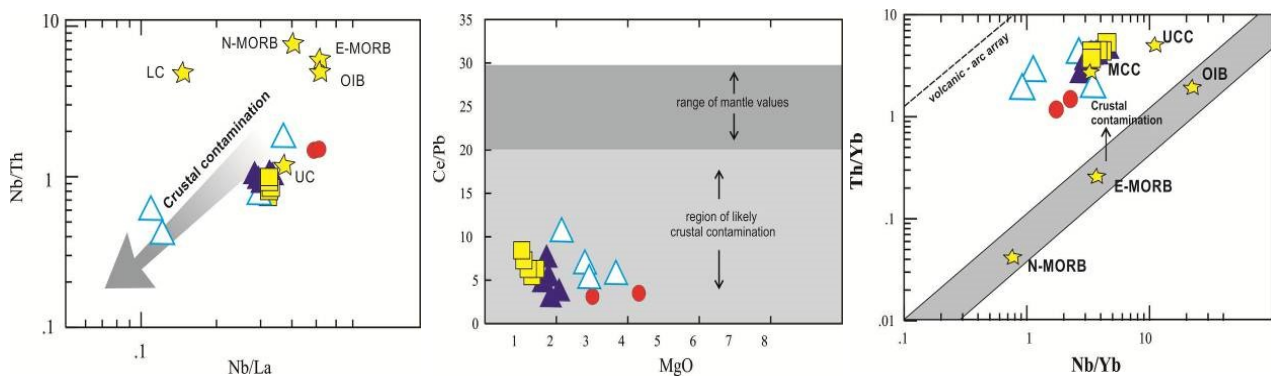


Fig 8. (a) Nb/La vs. Nb/Th diagram showing variable crustal contamination of the Kashmar granitoids. (b) Ce/Pb values are lower than those observed in MORB and their positive correlation with MgO suggests incorporation of materials from the upper (UCC) or lower continental crust (LCC) (crustal values from Rudnick and Fountain (1995); Taylor and McLennan (1995); Wedepohl (1995)). (c) Th/Yb vs. Nb/Yb diagram of the Kashmar granitoids (after Pearce (2008)). Average N-MORB, E-MORB, OIB are taken from (Sun and McDonough 1989); average middle crust (MCC) and upper crust (UCC) are selected from Rudnick and Fountain (1995) (symbols as for Figure 4).

partition coefficients of McKenzie and O'Nions (1991). Trace element ratio provide important constraints for the roles of mantle sources with composition of garnet- and spinel-bearing lherzolite (Baker et al. 1997). Partial melting of a spinel lherzolite mantle source does not change the Sm/Yb ratio because both Sm and Yb have similar partition coefficients, whereas it may decrease La/Sm ratios and Sm contents of the melts (Aldanmaz et al. 2000; Keskin 2005). The Yb is typically more compatible with garnet than clinopyroxene or spinel in which the Sm/Yb ratios in rocks should be sensitive to basalt source mineralogies. In the Sm/Yb versus La/Sm and Dy/Yb versus La/Yb diagrams (Fig 9), melt curves are drawn for spinel-lherzolite, garnet-lherzolite. Modal compositions of spinel-lherzolite (Ol 53%, Opx 27%, Cpx 17%, Sp 3%) and garnet-lherzolite (Ol 60%, Opx 20%, Cpx 10%, Grt 10%) are after Kinzler (1997) and Walter (1998). In the Sm/Yb versus La/Sm and Dy/Yb versus La/Yb diagrams (Fig 9), the Kashmar

gabbrodioritic rocks plot in the melting trends between 3% to 5% of partial melting of a spinel-lherzolite source. Therefore, the melts of the gabbrodioritic intrusions have been derived from a spinel-lherzolite mantle source.

#### 6.4. Possible depth of melting:

Variations of the thickness of the lithosphere and depth and degree of partial melting would affect trace-element compositions of basalts (McKenzie and O'Nions 1991; Behn and Grove 2015; Davies et al. 2015; Liu et al. 2016). Ellam (1992) demonstrate that Ce, Sm, and Yb concentrations can indicate a melt-segregation depth, in which Ce/Yb ratio is a sensitive indicator for changing lithospheric thickness. Because, differentiation via fractional crystallization does not influence the Ce/Yb ratio. In the Kashmar gabbrodiorites, Tk43 sample (as the parental magma), the Ce/Yb ratio indicates a final melt segregation depth of about 53 km (Fig 10).

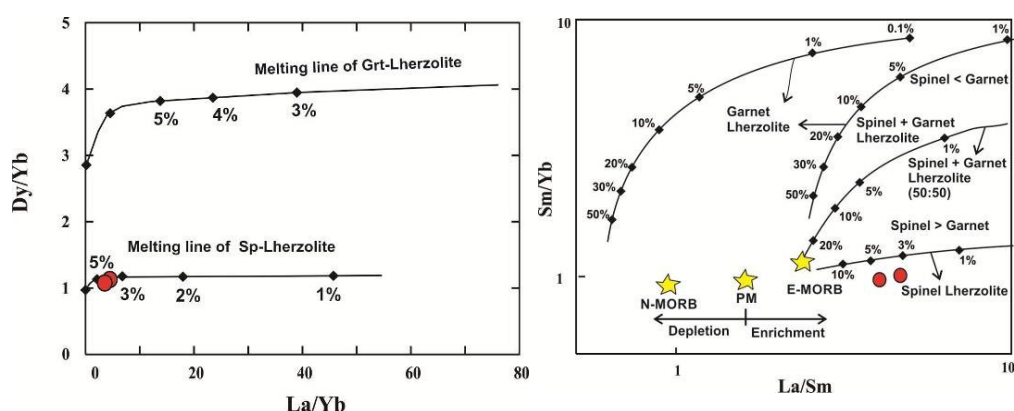


Fig. 9. (a) La/Yb vs. Dy/Yb and (b) La/Sm vs. Sm/Yb diagram to model the mantle melting degree for the Kashmar gabbrodioritic rocks. Partial melting curves were calculated using a modal batch melting model (Shaw 1970). La, Dy and Yb concentrations in the primitive mantle are taken from Hofmann (1988). Source mineralogy is 53% Ol, 27% Opx, 17% Cpx, 3% Sp for spinel-lherzolite and 60% Ol, 20% Opx, 10% Cpx, 10% for garnet peridotite. E-MORB, N-MORB and PM-Primitive mantle after (Sun and McDonough 1989). Mineral–melt distribution coefficients are from <http://earthref.org/KDD/>. (symbols as for Figure 4).

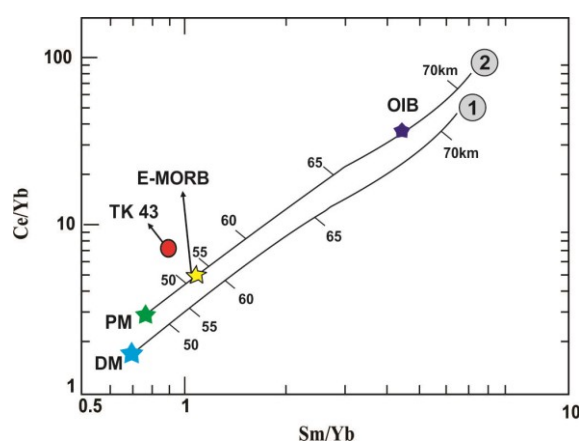


Fig. 10. Ce/Yb vs. Sm/Yb diagram used to show the depth of extraction of integrated pool melts produced by decompression fractional melting of a depleted asthenospheric mantle source (DM), and of the primitive mantle (PM), used as an estimate of a slightly enriched asthenospheric source.

## 5. Conclusion

Kashmar granitoids are composed of granites, granodiorites, monzodiorite and gabbrodiorites. The major and trace elements on Harker diagrams and REE chondrite-normalized patterns demonstrate that fractional crystallization of gabbrodioritic rocks probably could have played a significant role in formation of the more evolved rocks. Fractionation modeling involving the REEs reveals that the evolved granites was generated from the parental gabbrodiorite with high MgO, FeO, Cr, and Ni contents by fractional crystallization with about 60% residual liquid. Trace element ratios indicate that crustal contamination played an important role in petrogenesis of the granites. Trace element ratio modeling indicates that the gabbrodioritic rocks were produced by 3% to 5% partial melting of a spinel-lherzolite source at a ~53 km depth.

## Acknowledgements

The authors would like to acknowledge Islamic Azad University, Mashhad Branch (Iran), for financial support of this research project.

## References

- Alaminia Z, Karimpour MH, Homam SM, Finger F (2013) The magmatic record in the Arghash region (northeast Iran) and tectonic implications, *International Journal of Earth Sciences: Geologische Rundschau* 102:1603- 1625.
- Alavi M (1991) Tectonic map of the Middle East: Tehran, Geological Survey of Iran, Scale 1:5,000,000.
- Aldanmaz E, Pearce JA, Thirlwall M, Mitchell J (2000) Petrogenetic evolution of late Cenozoic, post-collision volcanism in western Anatolia, Turkey, *Journal of Volcanology and Geothermal Research* 102:67-95.
- Asiabanha A, Foden J (2012) Post-collisional transition from an extensional volcano-sedimentary basin to a

- continental arc in the Alborz Ranges, N-Iran, *Lithos* 148:98-111.
- Baker J, Menzies M, Thirlwall M, Macpherson C (1997) Petrogenesis of Quaternary intraplate volcanism, Sana'a, Yemen: implications for plume-lithosphere interaction and polybaric melt hybridization, *Journal of Petrology* 38:1359-1390.
- Behn MD, Grove TL (2015) Melting systematics in mid-ocean ridge basalts: Application of a plagioclase-spinel melting model to global variations in major element chemistry and crustal thickness, *Journal of Geophysical Research: Solid Earth* 120:4863-4886.
- Cox KG, Bell JD, Pankhurst RJ (1979) The interpretation of igneous rocks. G. Allen & Unwin.
- Davies D, Rawlinson N, Iaffaldano G, Campbell I (2015) Lithospheric controls on magma composition along Earth's longest continental hotspot track, *Nature* 525:511-514.
- Ellam R (1992) Lithospheric thickness as a control on basalt geochemistry, *Geology* 20:153-156.
- Fujimaki H, Tatsumoto M, Aoki Ki (1984) Partition coefficients of Hf, Zr, and REE between phenocrysts and groundmasses, *Journal of Geophysical Research: Solid Earth* 89(S02): B662-B672.
- Green NL (2006) Influence of slab thermal structure on basalt source regions and melting conditions: REE and HFSE constraints from the Garibaldi volcanic belt, northern Cascadia subduction system, *Lithos* 87:23-49.
- Gurenko AA, Chaussidon M (1995) Enriched and depleted primitive melts included in olivine from Icelandic tholeiites: Origin by continuous melting of a single mantle column, *Geochimica et cosmochimica acta* 59:2905-2917.
- Hanson GN (1978) The application of trace elements to the petrogenesis of igneous rocks of granitic composition, *Earth and Planetary Science Letters* 38:26-43.
- Hanson GN (1980) Rare earth elements in petrogenetic studies of igneous systems, *Annual Review of Earth and Planetary Sciences* 8: 371-406.
- Hofmann A, White W, Whitford D (1978) Geochemical constraints on mantle models: the case for a layered mantle, Carnegie Inst, *Washington Yearb* 77:548-562
- Hofmann AW (1988) Chemical differentiation of the earth - The relationship between mantle, continental crust, and oceanic crust, *Earth and Planetary Science Letters* 90:297-314.
- Johnson KTM (1998) Experimental determination of partition coefficients for rare earth and high-field-strength elements between clinopyroxene, garnet, and basaltic melt at high pressures, *Contributions to Mineralogy and Petrology* 133:60-68.
- Katz RF, Spiegelman M, Langmuir CH (2003) A new parameterization of hydrous mantle melting, *Geochemistry, Geophysics, Geosystems* 4(9).
- Keskin M (2005) Domal uplift and volcanism in a collision zone without a mantle plume: Evidence from Eastern Anatolia. www.MantlePlumes.org.
- Liu JQ, Chen LH, Zeng G, Wang XJ, Zhong Y, Yu X (2016) Lithospheric thickness controlled compositional variations in potassic basalts of Northeast China by melt-rock interactions, *Geophysical Research Letters* 43:2582-2589.
- McKenzie D, O'Nions R (1991) Partial melt distributions from inversion of rare earth element concentrations, *Journal of Petrology* 32:1021-1091.
- Monazzami Bagherzadeh R, Karimpour MH, Farmer GL, Stern C, Santos J, Rahimi B, Heidarian Shahri MR (2015) U-Pb zircon geochronology, petrochemical and Sr-Nd isotopic characteristic of Late Neoproterozoic granitoid of the Bornaward Complex (Bardaskan-NE Iran), *Journal of Asian Earth Sciences* 111:54-71.
- Munker C (2000) The isotope and trace element budget of the Cambrian Devil River arc system, New Zealand: identification of four source components, *Journal of Petrology* 41:759-788.
- Nakamura N (1974) Determination of REE, Ba, Fe, Mg, Na and K in carbonaceous and ordinary chondrites, *Geochimica et cosmochimica acta* 38:757-775.
- Pearce J, Peate D (1995) Tectonic implications of the composition of volcanic arc magmas, *Annual Review of Earth and Planetary Sciences* 23:251-286.
- Pearce JA (2008) Geochemical fingerprinting of oceanic basalts with applications to ophiolite classification and the search for Archean oceanic crust, *Lithos* 100:14-48
- Ramezani J, Tucker RD (2003) The Saghand region, central Iran: U-Pb geochronology, petrogenesis and implications for Gondwana tectonics, *American journal of science* 303:622-665.
- Rollinson HR (1993) Using geochemical data: evaluation, presentation, interpretation. Routledge.
- Rudnick RL, Fountain DM (1995) Nature and composition of the continental crust: a lower crustal perspective, *Reviews of geophysics* 33:267-309.
- Schmädicke E, Gose J, Reinhardt J, Will TM, Stalder R (2015) Garnet in cratonic and non-cratonic mantle and lower crustal xenoliths from southern Africa: Composition, water incorporation and geodynamic constraints, *Precambrian research* 270:285-299.
- Shafaii Moghadam H, Li X-H, Ling X-X, Santos JF, Stern RJ, Li Q-L, Ghorbani G (2015) Eocene Kashmar granitoids (NE Iran): petrogenetic constraints from U-Pb zircon geochronology and isotope geochemistry, *Lithos* 216:118-135.
- Shaw DM (1970) Trace element fractionation during anatexis, *Geochimica et cosmochimica acta* 34:237-243.
- Sobolev AV, Hofmann AW, Kuzmin DV, Yaxley GM, Arndt NT, Chung S-L, Danyushevsky LV, Elliott T, Frey FA, Garcia MO (2007) The amount of recycled crust in sources of mantle-derived melts, *Science* 316:412-417.
- Soltani A (2000) Geochemistry and geochronology of I-type granitoid rocks in the northeastern central Iran

- plate. Ph.D thesis, School of Geosciences, University of Wollongong.
- Stöcklin J, Nabavi M (1972) Tectonic Map of Iran. Geological Survey of Iran.
- Sun SS, McDonough W (1989) Chemical and isotopic systematics of oceanic basalts: implications for mantle composition and processes, *Geological Society, London, Special Publications* 42:313-345.
- Taylor SR, McLennan SM (1995) The geochemical evolution of the continental crust, *Reviews of Geophysics* 33:241-265.
- Wedepohl KH (1995) The composition of the continental crust, *Geochimica et cosmochimica acta* 59:1217-1232.
- Wilson M (1989a) *Igneous petrogenesis*. Springer.
- Wilson M (1989b) *Igneous petrogenesis: A global tectonic approach*: London, Unwyn Hyman.
- Zhao JH, Zhou MF (2007) Geochemistry of Neoproterozoic mafic intrusions in the Panzhihua district (Sichuan Province, SW China): implications for subduction-related metasomatism in the upper mantle, *Precambrian research* 152:27-47.